

# Spin-Dependent Transport Through An Interacting Quantum Dot

Ping Zhang<sup>1</sup>, Qi-Kun Xue<sup>1</sup>, Yu-Peng Wang<sup>1</sup>, X.C. Xie<sup>1,2</sup>

<sup>1</sup>*International Center of Quantum Structure and State Key Laboratory for Surface Physics, Institute of Physics, The Chinese Academy of Sciences, Beijing 100080, P.R. China*

<sup>2</sup>*Department of Physics, Oklahoma State University, Stillwater, OK 74078*

We study the nonequilibrium spin transport through a quantum dot containing two spin levels coupled to the magnetic electrodes. A formula for the spin-dependent current is obtained and is applied to discuss the linear conductance and magnetoresistance in the interacting regime, where the so-called Kondo effect arises. We show that the Kondo resonance and the correlation-induced spin splitting of the dot levels may be systematically controlled by internal magnetization in the electrodes. As a result, when the electrodes are in parallel magnetic configuration, the linear conductance is characterized by two spin-resolved peaks. Furthermore, the presence of the spin-flip process in the dot splits the Kondo resonance into three peaks.

PACS number(s): 73.23.-b, 73.63.-b, 75.25.+z

Key words: Kondo effect, magnetoresistance, quantum dot

Spin-polarized transport in magnetic nanostructures, in particular, single-electron tunneling in ferromagnetic (F) double junctions, has become a very active area of research, mainly because of its possible applications in information storage and processing devices [1]. In these junctions, the transport properties depend on the relative orientation of the magnetic moments of external electrodes. When the magnetic moments of the electrodes are antiparallel, the tunnel resistance increases. This is called as the tunnel magnetoresistance (TMR). When the central grain in double junctions is small enough to form a quantum dot (QD), the effects of the discrete quantized energy levels as well as Coulomb

blockade become significant, which has been considered theoretically and experimentally in the sequential tunneling regime [2,3,4,5,6,7,8,9,10,11].

In the low temperature regime, a more subtle effect of large charging energies is the creation of new states of many-body character at the Fermi level by the Kondo effect [13]. For a QD coupled to the normal (N) electrodes, the Kondo effect is well understood in and out of equilibrium [14,15,16,17]. It is a consequence of a special kind of high-order tunneling process in which the electron inside the QD tunnels out followed by an electron with opposite spin tunneling into the QD. The whole system forms a spin singlet state and the net magnetic moment in the QD is zero. For the F-QD-F system, a very important question is, what are the consequence and characteristics of the Kondo effect when the magnetic moments of the electrodes are taken into account?

In this Letter we have studied spin-dependent transport in an interacting QD coupled to two magnetic electrodes as shown schematically in Fig. 1. Different from the conventional Kondo problem in a N-QD-N system, here the characteristics induced by the strong electronic correlation is sensitive to the relative orientation of magnetization between the two electrodes, namely, the parallel and antiparallel configurations as shown in Fig. 1.

The model Hamiltonian for the F-QD-F system under consideration can be written as

$$\begin{aligned}
H = & \sum_{\sigma} \varepsilon_d d_{\sigma}^{\dagger} d_{\sigma} + U d_{\uparrow}^{\dagger} d_{\uparrow} d_{\downarrow}^{\dagger} d_{\downarrow} + R(d_{\uparrow}^{\dagger} d_{\downarrow} + \text{H.c.}) \\
& + \sum_{k\alpha \in L, R\sigma} \epsilon_{k\alpha\sigma} a_{k\alpha\sigma}^{\dagger} a_{k\alpha\sigma} + \sum_{k\alpha \in L, R\sigma} \left[ V_{k\alpha\sigma} a_{k\alpha\sigma}^{\dagger} d_{\alpha} + \text{H.c.} \right]
\end{aligned} \tag{1}$$

Here, the single particle energy  $\varepsilon_d$  is double degenerate in the spin index  $\sigma$ , and the interaction is included through the Coulomb repulsion  $U$ . The first two terms in  $H$  represent the correlated level of the QD, the third term is used to describe potential spin-orbit coupling which may cause the spin rotation of an electron while in the QD. The spin-flip mechanisms that are relevant to the GaAs-based QD have been studied recently [12]. The fourth term describes the free magnetic electrodes and the last term is the spin-dependent hybridization of the QD to the magnetic electrodes. Model (1) has been employed to study tunnel magnetoresistance in the sequential-tunneling regime [11].

Since the spin quantization axes in the electrodes are fixed by the internal magnetization of the magnets, the electrons tunnel into a superposition of spin-up and spin-down states. This coherence has to be taken into account when calculating current [20]. Technically, we introduce a spin rotation transformation  $d_{\uparrow(\downarrow)} = (1/\sqrt{2})(c_{\uparrow} \mp c_{\downarrow})$ , in terms of which the dot Hamiltonian in Eq. (1) is rewritten as  $\sum_{\sigma} \varepsilon_{c\sigma} c_{\sigma}^{\dagger} c_{\sigma} + U c_{\uparrow}^{\dagger} c_{\uparrow} c_{\downarrow}^{\dagger} c_{\downarrow}$  with  $\varepsilon_{c\sigma} = \varepsilon_d \pm R$  for up and down spins, respectively. The current through the left electrode can be calculated from the time evolution of the occupation number  $N_L = \sum_{k\sigma} a_{kL\sigma}^{\dagger} a_{kL\sigma}$  for electrons in the left electrode using nonequilibrium Green functions. The result is

$$J = e \langle \dot{N}_L \rangle = \frac{2e}{\hbar} \sum_k \int \frac{d\epsilon}{2\pi} \text{Tr}[\mathbf{V}_{kL} \mathbf{G}_{kL}^{<}(\epsilon)], \quad (2)$$

where we have defined the tunneling amplitude matrix

$$\mathbf{V}_{k\alpha} = \frac{1}{\sqrt{2}} \begin{pmatrix} V_{k\alpha\uparrow} & V_{k\alpha\downarrow} \\ -V_{k\alpha\uparrow} & V_{k\alpha\downarrow} \end{pmatrix}, \quad (3)$$

$\alpha = L, R$ , and lesser Green functions  $[\mathbf{G}_{kL}^{<}(t)]_{\sigma\sigma'} = i \langle a_{kL\sigma}^{\dagger}(0) c_{\sigma'}(t) \rangle$ . Next, we use Dyson's equation to calculate the non-equilibrium Green functions and express  $J$  by the Green functions  $\mathbf{G}_c$  of the dot as follows

$$J = \frac{e}{\hbar} \int \frac{d\epsilon}{2\pi} \text{Tr}\{\Gamma^L(\epsilon)[i\mathbf{G}_c^{<}(\epsilon) + f_L(\epsilon)\mathbf{A}(\epsilon)]\}, \quad (4)$$

where  $[\mathbf{G}_c^{<}(t)]_{\sigma\sigma'} = i \langle c_{\sigma'}^{\dagger}(t) c_{\sigma}(0) \rangle$  is the matrix expression for the lesser Green functions.  $\mathbf{A}(\epsilon) = i[\mathbf{G}_c^R(\epsilon) - \mathbf{G}_c^A(\epsilon)]$  is the spectral function.  $f_{\alpha}(\epsilon)$  is the Fermi-distribution function in the  $\alpha$  electrode, and

$$\Gamma^{\alpha}(\epsilon) = \frac{1}{2} \begin{pmatrix} \Gamma_{\uparrow}^{\alpha}(\epsilon) + \Gamma_{\downarrow}^{\alpha}(\epsilon) & \Gamma_{\downarrow}^{\alpha}(\epsilon) - \Gamma_{\uparrow}^{\alpha}(\epsilon) \\ \Gamma_{\downarrow}^{\alpha}(\epsilon) - \Gamma_{\uparrow}^{\alpha}(\epsilon) & \Gamma_{\uparrow}^{\alpha}(\epsilon) + \Gamma_{\downarrow}^{\alpha}(\epsilon) \end{pmatrix} \quad (5)$$

is the line-width matrix with  $\Gamma_{\sigma}^{\alpha}(\epsilon) = 2\pi \sum_{k \in \alpha} |V_{k\alpha\sigma}|^2 \delta(\epsilon - \epsilon_{k\alpha\sigma})$ . The spin-dependence of  $\Gamma_{\sigma}^{\alpha}(\epsilon)$  originates from the bulk magnetization of the electrodes.

In order to determine the retarded Green functions we choose the equation of motion (EOM) method. Although this method does not provide quantitative results in the Kondo

regime, it gives the qualitative feature both in equilibrium and nonequilibrium cases [16]. The method generates higher-order Green functions, which have to be truncated to close the equation. In the infinite- $U$  limit we obtain

$$\mathbf{G}_c^R(\epsilon) = [\epsilon \mathbf{I} - \hat{\varepsilon}_c - \Sigma_0^R(\epsilon) - \Sigma_1^R(\epsilon)]^{-1}(\mathbf{I} - \mathbf{n}_c) \quad (6)$$

where  $\mathbf{I}$  is a  $2 \times 2$  unit matrix,  $(\hat{\varepsilon}_c)_{\sigma\sigma'} = \delta_{\sigma\sigma'}\varepsilon_{c\sigma}$ ,  $\Sigma_0^R = -i(\mathbf{\Gamma}^L + \mathbf{\Gamma}^R)/2$  is the self-energy matrix due to the tunneling coupling between the electrodes and dot,  $\Sigma_1^R$  is due to the many-body correlation, with the matrix elements  $[\Sigma_1^R(\epsilon)]_{\sigma\sigma} = \sum_{k\alpha} [\frac{|V_{k\alpha\uparrow}|^2 f(\epsilon_{k\alpha\uparrow})}{\epsilon - \epsilon_{k\alpha\uparrow} - \varepsilon_{c\uparrow} + \varepsilon_{c\downarrow}} + \frac{|V_{k\alpha\downarrow}|^2 f(\epsilon_{k\alpha\downarrow})}{\epsilon - \epsilon_{k\alpha\downarrow} - \varepsilon_{c\uparrow} + \varepsilon_{c\downarrow}}]$ , and  $[\Sigma_1^R(\epsilon)]_{\sigma\bar{\sigma}} = \sum_{k\alpha} [\frac{|V_{k\alpha\uparrow}|^2 f(\epsilon_{k\alpha\uparrow})}{\epsilon - \epsilon_{k\alpha\uparrow}} - \frac{|V_{k\alpha\downarrow}|^2 f(\epsilon_{k\alpha\downarrow})}{\epsilon - \epsilon_{k\alpha\downarrow}}]$ ,  $(\mathbf{n}_c)_{\sigma\sigma'} = \delta_{\sigma\sigma'} \langle c_{\bar{\sigma}}^+ c_{\bar{\sigma}} \rangle$  must be calculated self-consistently.

To solve the lesser Green functions  $\mathbf{G}_c^<$  we generalize Ng's ansatz [19] to the present case. The interacting lesser and greater self-energies are assumed to be of the form  $\Sigma^{<, >} = \Sigma_0^{<, >} \mathbf{B}$ , where  $\mathbf{B}$  is a matrix to be determined by the condition  $\Sigma^< - \Sigma^> = \Sigma^R - \Sigma^A$ . This ansatz is exact in the non-interacting limit ( $U = 0$ ) and guarantees automatically the current conservation law. As a result one obtains  $\Sigma^< = \Sigma_0^< [\Sigma_0^R - \Sigma_0^A]^{-1} [\Sigma^R - \Sigma^A]$ . Using this ansatz,  $\mathbf{G}_c^<$  can be obtained by Keldysh equation  $\mathbf{G}_c^< = \mathbf{G}_c^R \Sigma^< \mathbf{G}_c^A$ . Substituting the expressions of the QD's Green functions in Eq. (4), defining  $\bar{\Sigma}^< = \mathbf{\Gamma}^R (\mathbf{\Gamma}^L + \mathbf{\Gamma}^R)^{-1} (\Sigma^R - \Sigma^A)$ , and after a straightforward calculation, one obtains a compact expression of the tunneling current

$$J = \frac{e}{\hbar} \int \frac{d\epsilon}{2\pi} \text{Tr}[\mathbf{\Gamma}^L \mathbf{G}_c^R \bar{\Sigma}^< \mathbf{G}_c^A] [f_L(\epsilon) - f_R(\epsilon)] \quad (7)$$

This expression generalizes the current formula in Ref. [16] to the spin-dependent Anderson model with additional spin-flip relaxation and allows one to describe the coherent spin transport through an interacting quantum dot coupled to magnetic electrodes.

In the following calculations, for simplicity we neglect the energy dependence in the tunneling matrix elements. The intrinsic linewidth of the dot energies has a form  $\Gamma_\sigma^\alpha(\epsilon) = \Gamma_\sigma^\alpha \theta(W - |\epsilon|)$  with the electrode band width  $2W \gg \max(k_B T, eV, \Gamma^\alpha)$ . We consider two magnetic configurations, namely, parallel and antiparallel configurations. When the magnetic electrodes are in parallel configuration, we assume that the spin-majority electrons are up ( $\sigma = \uparrow$ ) and the spin-minority electrons are down ( $\sigma = \downarrow$ ). We further assume

that in the antiparallel configuration the magnetization of the right electrode is reversed. Therefore the spin dependence of the coherent transport can be conveniently considered by introducing magnetic polarization factors  $p_L$  and  $p_R$  for the left and right barriers, respectively.  $\Gamma_{\uparrow(\downarrow)}^L = \Gamma_0(1 \pm p_L)$ ,  $\Gamma_{\uparrow(\downarrow)}^R = \alpha\Gamma_0(1 \pm p_R)$  is for the parallel configuration, and  $\Gamma_{\uparrow(\downarrow)}^R = \alpha\Gamma_0(1 \mp p_R)$  for the antiparallel configuration.  $\Gamma_0$  describes the coupling between the quantum dot and the left electrode without internal magnetization and  $\alpha$  denotes tunnel asymmetry between the left and right barriers. In this work we assume the symmetric barriers, i.e.,  $\alpha = 1$ ,  $p_L = p_R = p$ .

The spin-resolved spectral densities are calculated via the relation  $\rho_{\uparrow(\downarrow)}(\epsilon) = -\frac{1}{\pi} \text{Im}\{(\mathbf{G}_c^R)_{\uparrow\uparrow} + (\mathbf{G}_c^R)_{\downarrow\downarrow} \mp (\mathbf{G}_c^R)_{\uparrow\downarrow} \mp (\mathbf{G}_c^R)_{\downarrow\uparrow}\}$ . Figure 2 shows the behavior of the spectral densities in parallel and antiparallel magnetic configurations, which will be used to discuss the conductance results below. The Kondo resonance for each spin is clearly manifested by a sharp peak at  $\epsilon = 0$  (the chemical potential is set to be zero) in spectral densities for both magnetic configurations. However, the peak shape is sensitive to the magnetic configurations of the electrodes. As observed from Fig. 2(a), in parallel configuration the excitation characteristics of the spectral densities are remarkably different from the normal case in two prominent ways: (i) the Kondo resonance for down spin is enhanced, while the up-spin resonance is suppressed; (ii) interestingly, the broad single-particle resonances shift away from the dot level  $\epsilon_d$ , but in opposite directions for different spins. The excitations for the down spin shifts towards higher energy, while it shifts to lower energy for the up spin. This splitting is due to the spin-dependence of the interacting self-energy matrix  $\Sigma_1^R(\epsilon)$ , whose real part is different for the up and down spins and sensitive to the values of the spin polarization factor  $p$ . From the expression of  $\Sigma_1^R(\epsilon)$ , the renormalized spin levels  $\tilde{\epsilon}_{d\sigma}$  are given by the self-consistent equation

$$\begin{aligned}\tilde{\epsilon}_{d\sigma} &= \epsilon_d + \sum_{k\alpha} \frac{|V_{k\alpha\bar{\sigma}}|^2 f(\epsilon_{k\alpha\bar{\sigma}})}{\tilde{\epsilon}_{d\sigma} - \epsilon_{k\alpha\bar{\sigma}}} \\ &= \epsilon_d + \sum_{\alpha} \frac{\Gamma_{\bar{\sigma}}^{\alpha}}{2\pi} \left\{ \ln \frac{2\pi k_B T}{W} + \text{Re} \Psi \left[ \frac{1}{2} - i \frac{\tilde{\epsilon}_d - \mu_{\alpha}}{2\pi k_B T} \right] \right\},\end{aligned}\quad (8)$$

where  $\Psi$  is the digamma function. The result of Eq. (8) is shown in the inset of Fig. 2 (a),

where the dressed dot levels  $\tilde{\varepsilon}_{d\sigma}$  are plotted as a function of  $p$ . This spin splitting of the dot levels in the interacting regime due to the magnetic properties of the electrodes leads to essential changes in the transport properties (see below). In addition, as  $p$  increases, the spectral weight of  $\rho_{\downarrow}(\epsilon)$  goes up, while the spectral weight of  $\rho_{\uparrow}(\epsilon)$  is reduced. Thus a net magnetic moment is induced by the magnetic coupling. In the case of antiparallel configuration, the spectral densities of two spins are identical and the Kondo peak is not influenced by the presence of magnetic polarization of the electrodes [see Fig. 2(b)].

The level dressing and Kondo resonances in Fig. 2(a) are suppressed when taking into account the spin-flip process. Remarkably, it shows in Fig. 3(a) that a large spin-flip transition  $R$  splits the original Kondo peak into *three* well-defined peaks. As seen from the expression of  $\Sigma_1^R(\epsilon)$ , besides the peak at  $\epsilon = 0$ , the additional two peaks appear at  $\epsilon = \pm R$ , respectively. It is different from the antiparallel case with symmetric barriers, in which, as in the normal case, only the two Kondo peaks evolves from the presence of the spin-flip process [see Fig. 3(b)].

The dramatic changes in the spectral densities when rotating magnetic moments of the electrodes from parallel to antiparallel configuration suggests substantial different transport properties for these two configurations. Figure 4 shows the linear response conductance  $G$  as a function of  $\varepsilon_d$ , which can be tuned via the external gate voltage, for different temperatures. In the antiparallel configuration, as observed from Fig. 4(a), the temperature dependence of the conductance is similar to the normal case although with a lower amplitude: the Kondo resonance broadens the conductance peak and saturates the peak amplitude at low temperatures. In addition, the peak shape remains nearly symmetric over a broad range of temperatures. In the parallel configuration, however, the conductance peak becomes asymmetric with decreasing temperature as shown in Fig. 4(b). This asymmetry is even more pronounced in the spin-resolved conductance  $G_{\sigma}$  [see the inset of Fig. 4(b)]. The peak splitting in  $G_{\uparrow}$  and  $G_{\downarrow}$  is in the same manner as shown in Fig. 2 due to the magnetic dressing of spin levels. Thus their superposition results in a double-peak structure at low temperatures and for large  $p$  as shown in Fig. 4(b) (dotted line). The main peak with larger

amplitude is dominated by the up-spin resonance, while the other peak with lower amplitude nearly comes from the down-spin resonance. This novel spin filtering effect is fully caused by the interplay between the dot correlation and the magnetic coupling. When spin-flip transition is included, as shown in Fig. 4(c), the splitting of the conductance is suppressed.

To describe the dramatic change of  $G$  when the magnetic moments in the electrodes are rotated from antiparallel to parallel configuration, we define the linear magnetoresistance as  $MR = (G_p - G_{ap})/G_{ap}$ , where  $G_p$  and  $G_{ap}$  are the linear conductance in the parallel and the antiparallel configurations, respectively. Figure 5 shows the magnetoresistance as a function of  $\varepsilon_d$  for different temperatures. One can see that when the dot level is far from resonance, the magnetoresistances approach to the same value for different temperatures, coinciding with the non-interacting case. At low temperatures, however, dramatic changes occur in the resonant tunneling regime. The magnetoresistance develops into a dip with a negative value. This means that the linear magnetoresistance significantly decreases and even changes its sign at low gate voltages. In the empty orbital regime where the dot level is higher than the chemical potential of the electrodes, the magnetoresistance may be enhanced to a value as large as 160%.

In summary, using Anderson model, it is shown that the magnetic moment arrangement in the electrodes plays an essential role in spin-dependent transport of a F-QD-F system in the interacting regime. For parallel magnetic configuration, the Kondo resonance and QD energy levels can be controlled by the magnetic polarization in the electrodes. Consequently, the linear conductance appears as a spin-resolved double-peak structure and a net magnetic moment emerges in the QD. The spin-flip process in the QD results in a splitting of the Kondo peak into three peaks. We expect these results are useful in exploiting the role of electronic correlation in spintronics.

This work is supported by CNSF under Grant No. 69625608 and by US-DOE.

*Note added.*—After the work was completed, we noticed that Kondo problem in TMR has also been considered by Sergueev *et al.* [21]. However, they did not discuss spin splitting of the conductance and spin-flip effects, which compose essential points in this paper.

- 
- [1] For recent reviews see G. A. Prinz, *Science* **282**, 1660 (1998); M. Johnson, *IEEE Spectr.* **37**(2), 33 (2000).
- [2] K. Ono, H. Shimada, S. Kobayashi, and Y. Ootuka, *J. Phys. Soc. Jpn.* **65**, 3449 (1996); K. ono, H. Shimada, and Y. Ootuka, *ibid.* **66**, 1261 (1997).
- [3] L.F. Schelp *et al.*, *Phys. Rev. B* **56**, R5747 (1997).
- [4] S. Takahashi and S. Maekawa, *Phys. Rev. Lett.* **80**, 1758 (1998).
- [5] X.H. Wang and A. Brataas, *Phys. Rev. Lett.* **83**, 5138 (1999).
- [6] J. Barnas and A. Fert, *Phys. Rev. Lett.* **80**, 1058 (1998).
- [7] J. Martinek, J. Barnas, G. Michalek, B.R. Bulka, and A. Fert, *J. Magn. Magn. Mater.* **207**, L1 (1999).
- [8] B.R. Bulka, J. Martinek, G. Michalek, and J. Barnas, *Phys. Rev. B* **60**, 12246 (1999).
- [9] J. Barnas, J. Martinek, G. Michalek, B.R. Bulka, and A. Fert, *Phys. Rev. B* **62**, 12363 (2000).
- [10] B.R. Bulka, *Phys. Rev. B* **62**, 1186 (2000).
- [11] W. Rudziński and J. Barnas, *Phys. Rev. B* **64**, 085318 (2001).
- [12] A.V. Khaetskii and Y.V. Nazarov, *Phys. Rev. B* **61**, 12639 (2000); A.V. Khaetskii, *Physica E* **10**, 27 (2001).
- [13] A.C. Hewson, *The Kondo Problem to Heavy Fermions* (Cambridge University Press, Cambridge, England, 1993).
- [14] L.I. Glazman and M.E. Raikh, *JETP Lett.* **47**, 452 (1988).
- [15] T.-K. Ng and P.A. Lee, *Phys. Rev. Lett.* **61**, 1768 (1988).



- [16] Y. Meir, N.S. Wingreen, and P.A. Lee, Phys. Rev. Lett. **70**, 2601 (1993).
- [17] N.S. Wingreen and Y. Meir, Phys. Rev. B **49**, 11040 (1994).
- [18] Y. Meir and N.S. Wingreen, Phys. Rev. Lett. **68**, 2512 (1992).
- [19] T.-K. Ng, Phys. Rev. Lett. **76**, 487 (1996).
- [20] G. Usaj and H.U. Baranger, Phys. Rev. B **63**, 184418 (2001).
- [21] N. Sergueev, Q.-F. Sun, H. Guo, B.G. Wang, and J. Wang, Phys. Rev. B **65**, 165303 (2002).

## Figure captions

Fig. 1. Schematic plot of the F-QD-F system considered in this work.

Fig. 2.  $\rho_{\uparrow}(\epsilon)$  (solid line) and  $\rho_{\downarrow}(\epsilon)$  (dotted line) as a function of  $\epsilon$  in the (a) parallel, and (b) antiparallel magnetic configurations for  $p = 0.5$ ,  $k_B T = 0.02\Gamma_0$ ,  $\varepsilon_d = -4\Gamma_0$ , and  $R = 0$ . Inset in (a) indicates spin splitting of the dot levels as a function of  $p$ .

Fig. 3.  $\rho(\epsilon)$  as a function of  $\epsilon$  in the (a) parallel, and (b) antiparallel magnetic configurations with  $R = 0.2\Gamma_0$ . Other parameters are the same as in Fig. 2.

Fig. 4. Linear conductance  $G$  as a function of  $\varepsilon_d$  in the (a) antiparallel, and (b) parallel magnetic configurations in the absence of spin-flip process with  $p = 0.5$ . Inset indicates spin-resolved conductance  $G_{\uparrow}$  and  $G_{\downarrow}$ . The effect of of intradot spin-flipping on the parallel conductance is shown in (c).

Fig. 5. Linear magnetoresistance as a function of  $\varepsilon_d$  for several values of temperature. Other parameters are the same as in Fig. 4.

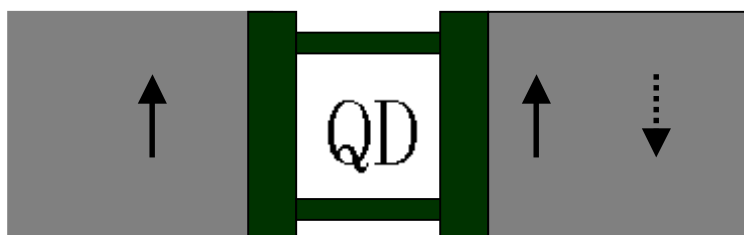


Fig.1

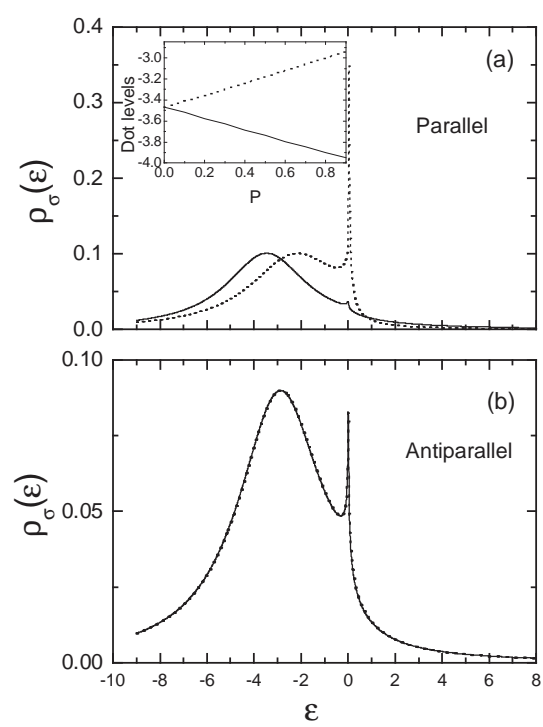


Fig. 2

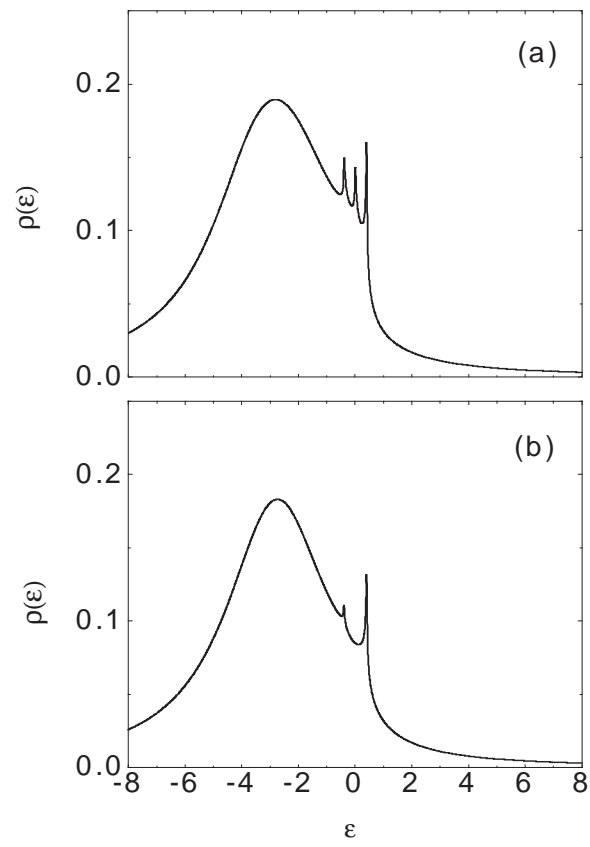


Fig. 3

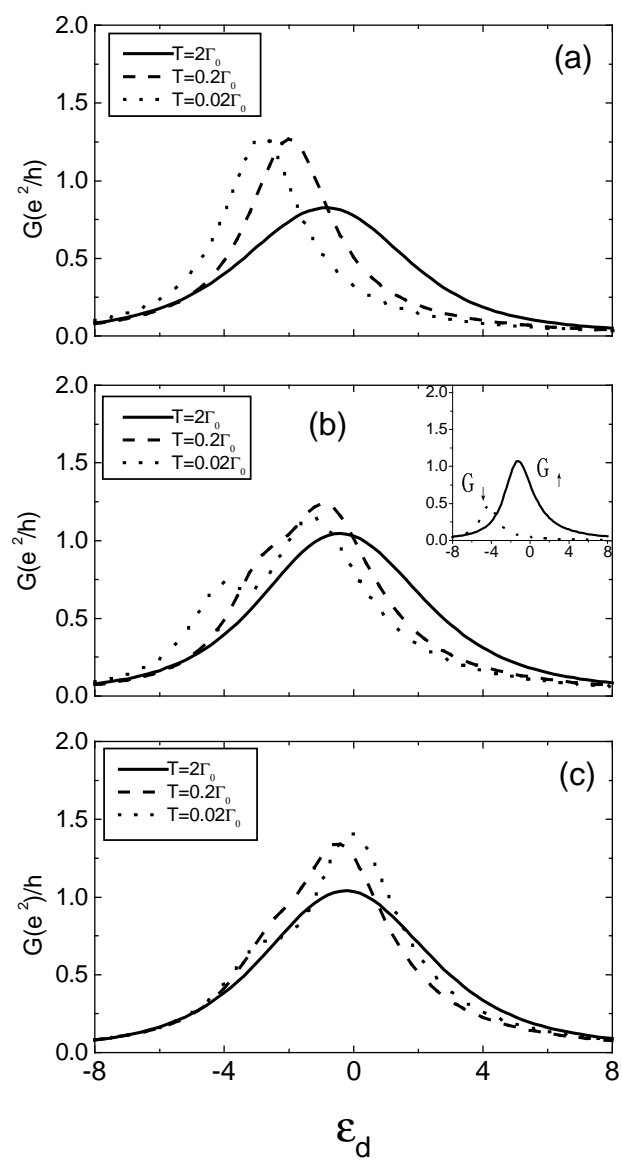


Fig.4

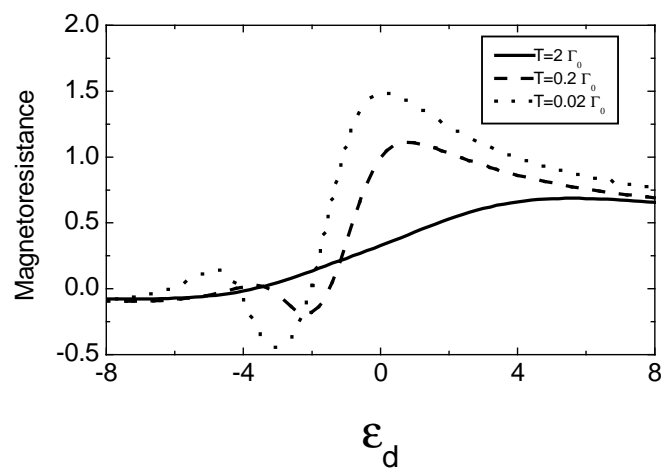


Fig.5